Received: 24 July 2018 | Revised: 19 March 2019 | Accepted: 29 March 2019

DOI: 10.1111/avsc.12441

RESEARCH ARTICLE

Applied Vegetation Science
IAVS

Cumulative disturbances to assess forest degradation using spectral unmixing in the northeastern Amazon

Ali Fadhil Hasan[1] | François Laurent[1] | François Messner[1] | Clément Bourgoin[2] | Lilian Blanc[2]

[1]UMR ESO, Le Mans Université, Le Mans, France

[2]UR Forests and Societies, CIRAD Occitanie-Montpellier, Montpellier, France

Correspondence
François Laurent, UMR ESO, Le Mans Université, Le Mans, France.
Email: francois.laurent@univ-lemans.fr

Funding information
Agence Nationale de la Recherche; award number: ANR-13-AGRO-0003
European Union; award number: H2020-MSCA-RISE-2015 ODYSSEA project.

Co-ordinating Editor: Duccio Rocchini

Abstract

Question: Tropical forests are subject to disturbances by logging, gathering of fuelwood, and fires. Can degradation trajectories (i.e. cumulative disturbances events over a period of timer) be identified using remote-sensing Landsat time series?

Location: Paragominas (Pará, Brazil), a municipality covering 19,395 km² in the northeastern Amazon.

Methods: We used Landsat annual imagery from 2000 to 2015 and spectral mixture analysis to derive time series of the fraction of soil (S), active photosynthetic vegetation (PV), and non-photosynthetic vegetation (senescent) (NPV) indicators.

Results: The NPV values over a 16-year period revealed five different degradation trajectories (i.e., cumulative disturbances in space and over time): undisturbed forest, selectively logged forest (with a management plan), overlogged forest (no management plan), overlogged forest (charcoal production) and burned forest. The variance of NPV calculated per pixel over the same period is useful to map forest degradation over Paragominas municipality, highlighting the role of disturbance factors (logging, fuelwood gathering and fire).

Conclusions: The fractional cover of NPV obtained from spectral mixture analysis can be used to differentiate degradation trajectories and to map forest degradation.

KEYWORDS
Amazon, CLASlite, forest degradation, landsat time, logging, remote sensing, series

1 | INTRODUCTION

Since the 1960s, the Brazilian Amazon has undergone large-scale deforestation for the purpose of cattle farming, cropping, mining and urbanization (Cardille, & Foley, 2003; Ewers, Laurance, & Souza, 2008; Garcia, Soares-Filho, & Sawyer, 2007; Gibbs et al., 2010; Théry, 1997; Velasco Gomez et al., 2015). Deforestation first occurred along the eastern and southern borders of the rainforest, which was called the “agricultural frontier” or “arc of deforestation” (Rodrigues et al., 2009). The deforestation process is now slowing down under the scrutiny of international organizations and the government. From 2004 to 2014, the enforcement of environmental control, credit restriction for farms pursuing illegal deforestation and commitments by supply chains have significantly reduced the rate of deforestation (Gibbs et al., 2016; Nepstad et al., 2014; Tritsch & Arvor, 2016), although in 2015 and 2016, deforestation started to increase again (Fearnside, 2017). However, the Amazon forest is not only threatened by deforestation, but also by degradation. As shown by Souza et al., (2013), as deforestation in the Brazilian Amazon declined, forest degradation increased from 2000 to 2010 (PRODES and DEGRAD programs developed by INPE, Brazil's National Institute for Space Research).

Forest degradation is defined as a decrease in tree density resulting in a change in forest structure, with loss of the functions, biodiversity or biomass normally associated with — and locally expected

 © 2019 International Association for Vegetation Science

from — natural forest (ITTO, 2002). Forest degradation reduces the capacity of a forest to provide goods and services (FAO, 2002) including climate change mitigation (Baccini et al., 2017; Bustamante et al., 2016; Thompson et al., 2013). Large areas of rainforest all over the world are affected by forest degradation (Alves, Morton, Batistella, Roberts, & Souza, 2009). In the Brazilian Amazon, the INPE classified about 103,000 km² of forest as degraded due to illegal selective logging and fires between 2007 and 2013, which represents almost twice the extent of deforestation over the same period (Aguiar et al., 2016).

Degradation can have natural causes such as climate change, but is more commonly associated with local human activities that have medium- and long-term consequences. In the Brazilian Amazon, forest fires, fragmentation due to the opening up of agricultural lands, unsustainable selective logging, gathering fuelwood for charcoal production and livestock grazing are the main processes responsible for forest degradation (Alves et al., 2009; Ferreira et al., 2015; Hosonuma et al., 2012; Matricardi, Skole, Cochrane, Qi, & Chomentowski, 2005; Matricardi, Skole, Pedlowski, Chomentowski, & Fernandes, 2010; Pinheiro et al., 2016). Fires, even of low intensity, alter forest composition and structure (Xaud, Martins, & dos Santos, 2013). Selective logging leaves gaps in the forest, roads, and injured remaining trees, whose mortality contributes significantly to biomass losses following logging (Sist, Mazzei, Blanc, & Rutishauser, 2014). Although cleared areas are closed by secondary vegetation following the harvest of timber or damage caused by fire, secondary vegetation does not have the same characteristics as the original vegetation and requires decades or even centuries to recover from biomass losses (Asner et al., 2005; Gerwing, 2002).

It is important to assess forest degradation by remote sensing and to identify the causes of degradation over large areas in order to improve their management, to establish priorities, and to implement actions to stop and reverse the degradation process (Asner, Rudel, Aide, Defries, & Emerson, 2009; FAO, 2011, p. 81; Lamb & Gilmour, 2003, p. 110). However, identifying and characterizing forest degradation is difficult using remote sensing because degradation is less visible than large-scale clearing combined with land use change, and because the spectral signature of logging and forest fires changes rapidly as the gaps close due to the growth of secondary vegetation, even if damage to the forest has consequences for the forest structure. Forest degradation is a medium- or long-term process and consequently requires specific remote-sensing analysis and monitoring every year (Lambin, 1999).

A number of authors have used remote sensing to analyze forest degradation using different sensors (Matricardi et al., 2010, 2005; Monteiro, Souza, & Barreto, 2003; Souza et al., 2013; Souza, Firestone, Silva & Roberts, 2003). The high frequency of MODIS imagery enables efficient mapping of burned forest areas, and the MODIS multi-temporal dataset enables differentiation between deforestation and degradation processes when they affect large areas (Shimabukuro, Beuchle, Grecchi, & Achard, 2014). DETER with MODIS images (250 m) and DETER-B with AWIFS data (56 m) are tools developed by INPE for low-resolution sensors to detect deforestation and large clearings caused by forest cutting or burning in the Brazilian Amazon at near-real time (Diniz et al., 2015). The INPE conceived another method to specifically monitor forest degradation, called DEGRAD (obt.inpe.br), which makes it possible to detect disturbances affecting areas of more than 6.25 ha (INPE, 2008). Annual results have been available since 2007. In some areas of public land under forestry concessions, a more accurate resolution has been processed by INPE for the DETEX project (Selective Logging Detection Project). It is based on CCD/CBERS-2. However, the use of low spatial resolution tools limits the identification of the selective logging processes, by not detecting the small clearings that are used to temporarily store logs (log landings). And the more important, the tools are not designed to identify the consequences of this type of damage to forests in the medium and long term, they detect more the disturbance than the degradation.

In the Peruvian Amazon, (DeVries et al., 2015) tracked forest changes using dense Landsat time series, and detected disturbance–regrowth dynamics with high spatial and temporal resolution. With Landsat, SPOT or other medium-resolution sensors, fraction images of soil cover derived from linear mixture models make it possible to detect small clearings. For this purpose, non-photosynthetic vegetation and shade fractions have been used to estimate the levels of forest degradation caused by burning (Cochrane, 1998). The Carnegie Landsat Analysis System (CLASlite) is a tool based on a linear mixture model and decision tree classification designed to assess forest disturbances over large areas of the Brazilian Amazon (Asner et al., 2005, 2006; Dlamini, 2017; Matricardi et al., 2005; Monteiro et al., 2003; Souza & Barreto, 2000; Souza et al., 2003). CLASlite makes it possible to distinguish the fractions of photosynthetic vegetation (PV), non-photosynthetic vegetation (NPV) and bare substrate (S). CLASlite-based analysis is an approach to monitor forest degradation that can be used to detect selective logging (Chicas, Omine, & Saqui, 2016). However, CLASlite has rarely been used to assess the cumulative impacts of degradation processes, and hence their medium- and long-term effects on forest degradation. In a region of Mato Grosso heavily impacted by deforestation and selective logging, Grecchi et al. (2017) investigated the annual changes due to forest disturbance caused by selective logging using a Landsat multi-temporal dataset over a 15-year period processed with spectral mixture analysis. These authors reported on the areas affected by selective logging using a regular grid with 300 m × 300 m cells. For each grid cell and each single year, the percentages of forest, deforested areas and “logging” pixels were computed, and the grid cells were classified in relation to the intensity of the disturbance. The authors also assessed the number of times a grid cell was detected as “disturbed” over the 15-year period to characterize the medium-term degradation process. Tritsch et al. (2016) analyzed multi-temporal Landsat images with CLASlite to detect logging activity based on canopy openings and to monitor the trajectories of forest disturbance over time. Using principal component analysis and hierarchical cluster analysis, they classified logging plots in five disturbance patterns in terms of logging intensity and frequency. They characterized forest disturbance trajectories over time, from legally certified logging to high overlogging. In the same area, which represents an old Amazon agricultural frontier with a mosaic of degraded forest, among a number of other variables, Bourgoin et al. (2018) classified Landsat spectral unmixing using CLASlite and mid-infrared variables as the most robust and most explanatory variables of the aboveground biomass remaining in degraded forest. With these advances, there is now a need to study the cumulative impacts of forest damage over time.

The aim of the present study was to evaluate the capacity of vegetation fractions resulting from spectral unmixing and their variance during a time series to identify the intensity of medium- and long-term forest degradation based on accumulated damage. We selected Paragominas municipality, an agricultural frontier area in the Brazilian Amazon that has been subject to recurrent logging and fire. Our first objective was to identify, at pixel scale, disturbance events that occurred over a 15-year period from fractions of PV, NPV and bare substrate, using Landsat time series and the CLASlite platform. Our second objective was to analyze, at pixel and plot scale, the degradation and recovery trajectories to better understand changes in vegetation activity according to different disturbance factors: logging for timber, forest fire and gathering fuelwood. Our third objective was to map the intensity of forest degradation resulting from the 15-year period of disturbances, at the municipal scale. In the rest of the paper, we use the term "disturbance" to cover the actions of forest cover disturbance and the term "degradation" to cover the cumulative effects of these disturbances on the state of the forest.

2 | STUDY AREA

Paragominas is a municipality in the eastern Amazon crossed by the federal road between Belém and Brasilia (BR-010) (Figure 1). The municipality was founded in 1965 and now covers 19,395 km². The climate is tropical (type Aw, according to the Köppen classification), with an average annual temperature of 26.3°C and a mean relative humidity of 81%. Average annual rainfall recorded at Paragominas station between 1992 and 2010 was 1,693 mm (Andrade, 2011). Eighty-three percent of the annual precipitation falls in the rainy season from December to May. From June to November, mean monthly rainfall is less than 100 mm/month. Landforms consist of plateaus at an elevation of 160–190 m above sea level, separated by valleys up to several kilometers wide. The most prevalent soils are Ferralsols, clayey on the plateaus and sandy in the valleys (Laurent, Poccard-Chapuis, Plassin, & Pimentel Martinez, 2016). The natural vegetation is a dense tropical moist forest, but 45% of the study area has been deforested since the 1960s (INPE, 2010), mainly for cattle farming, and since the 2000s for soybean and maize cropping (Piketty et al., 2015). The forests have been degraded by the extraction of timber and charcoal production.

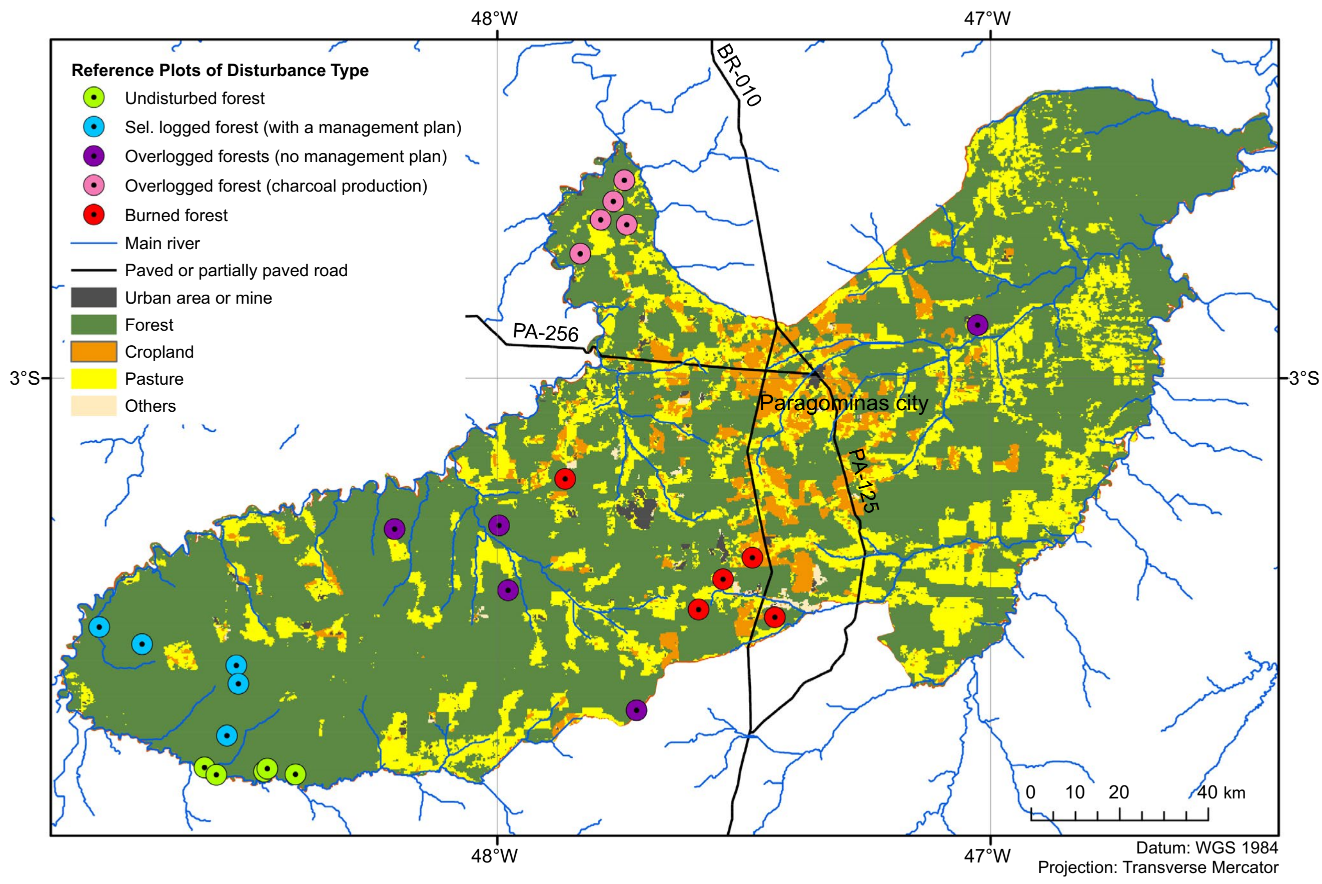

FIGURE 1 Location of the 25 reference plots characterizing the five forest degradation types in the municipality of Paragominas [Colour figure can be viewed at wileyonlinelibrary.com]

In 1990, the municipality was the largest timber production center in Brazil (Verissimo, Barreto, Mattos, Tarifa, & Uhl, 1992). In 2006, Paragominas was put on the blacklist for the illegal deforestation. In response to the sanctions, the local stakeholders and the majority of farmers decided to respect the environmental laws by changing the development model of the territory. Since then, Paragominas municipality has been involved in reducing deforestation and mapping farms' protected areas, labeled by the Green Municipality program (Laurent et al., 2017). Little is known about the degradation status of the remaining forests, however, and their management is an open question.

3 | METHODS

3.1 | Field observations and identification of reference plots

Two field missions in May and August 2015 made it possible to build a typology of degraded forests using GPS data acquisition and qualitative descriptions (see further details in Bourgoin et al., 2018). Based on the spatial distribution of the data, Google Earth images and Esri World Imagery (July 2016), the plot reference database was completed by visual interpretation of disturbance impacts.

We identified five reference plots for each type of forest degradation (Figure 1). Including all the area affected by similar management or by fire meant the plots differ in size. Plots of undisturbed forests and logged forests with a management plan were selected in the western part of the municipality, in the fazenda Rio Capim owned by CIKEL-Brazil Verde. Forest management has been under Forest Stewardship Certification since 2001. The plots of overlogged forest for charcoal production are located in the northern part of the municipality. In these forests, almost all trees with a diameter at breast height >10 cm have been removed. Overlogged forest (no management plan) and burned forest plots are scattered throughout the municipality. In the overlogged forests (no management plan), a few tall trees with a large diameter of non-commercial species are still present. The burned forests are characterized by a high abundance of dead standing trees compared to other forest types. The mean surface area of the five plots was 38.1 ha (min: 24; max: 58) for the undisturbed forest, 290.5 ha (min: 85; max: 883) for selectively logged forest, 317.6 ha (min: 178; max: 610) for overlogged forests (no management plan), 169.2 ha (min: 74; max: 216) for overlogged forest (charcoal production) and 277.6 (min: 165; max: 358) for burned forest. Based on the Google Earth archive, we reconstructed the history of disturbance events between 2000 and 2015 for each of the reference plots. We used this information for the validation of the NPV time series (see Results).

3.2 | Processing of remote-sensing images

CLASlite is a software package designed to automatically identify deforestation and forest disturbance on satellite imagery. It is used to convert raw satellite images into fractional cover maps of live vegetation canopy, dead vegetation, and bare surface. These fractional covers are core determinants of forest composition, structure, biomass, physiology and biogeochemical processes (Asner et al., 2005; Oliveira et al., 2007). The method requires "libraries" of spectral end-members for each of three relevant surface cover types: PV (fractional cover PV), NPV (fractional cover NPV), and bare substrate (fractional cover S). Spectral properties of the PV band are specific to leaf photosynthetic pigments, canopy water content, and the amount of foliage in the canopy. Spectral properties of the NPV band are associated with dried carbon compounds in dead leaves and exposed wood. The S band represents exposed mineral soil, rock outcrops, buildings and roads. The fractional cover of each band for each pixel is provided by a Monte Carlo method (Automated Monte Carlo Unmixing Process), where the possible combinations of the endmember spectra are pre-computed with libraries derived from extensive field databases and satellite imagery provided with CLASlite. Each image pixel is decomposed using the following linear equation (Asner, Knapp, Balaji, & Paez-Acosta, 2009):

$$\begin{aligned} &\mathrm{P}(\lambda)\mathrm{pixel} = \sum[\mathrm{Ce}\cdot\mathrm{P}(\lambda)\mathrm{e}] + \varepsilon = \\ &[\mathrm{CPV}\cdot\mathrm{P}(\lambda)\mathrm{pv} + \mathrm{Cnpv}\cdot\mathrm{P}(\lambda)\mathrm{npv} + \mathrm{Csubstrate}\cdot\mathrm{P}(\lambda)\ \mathrm{substrate}] + \varepsilon \end{aligned} \tag{1}$$

where $P(\lambda)_e$ is the reflectance value of the observed pixel at wavelength λ and C_{PV}, C_{NPV} and C_S are the percentages of fractional covers for the aforementioned principal constituents or endmembers, $P(\lambda)_{PV}$, $P(\lambda)_{NPV}$ and $P(\lambda)_S$ being the corresponding reflectance at wavelength λ for every one of the three endmembers considered, and (ε) is an error term.

The three spectral indicators of fractional covers (S, PV and NPV) are expressed as a percentage (0%–100%) for each pixel. A specific color is assigned to each fractional cover: PV is in green. NPV is in blue, substrate (S) is in red (Asner, Rudel et al., 2009). Other colors like magenta or orange represent interactions between the bands. Spatial patterns of CLASlite bands revealed differences between types of disturbance: a system of regular geometrically shaped gaps and a network of roads to extract timbers with high S and NPV values in the selective logging areas (Asner, Keller, Pereira, Zweede, & Silva, 2004), while the forest fire and charcoal production areas were randomly shaped, with homogeneous distribution of NPV and without S band.

Landsat Operational Land Imager (OLI), Enhanced Thematic Mapper (ETM+) and Thematic Mapper (TM) images were selected on the earthexplorer.usgs.gov website to form a time series during the dry season between 2000 and 2015. To cover the entire Paragominas municipality, four images were used with path and row numbers (222–26, 222–63, 223–62, 223–63). The Landsat imagery from 2000 to 2015 was analyzed with CLASlite through the calibration, pre-processing, atmospheric correction, cloud masking and Monte Carlo Spectral Mixture Analysis (Figure 2). CLASlite uses the 6S radiative transfer model (CLASlite, 2014; Vermote, Tanre, Deuze, Herman, & Morcette, 1997), which simulates the Earth's atmosphere in each satellite image. The raw image is corrected by removing the estimated model of the atmosphere, resulting in an image of surface reflectance. One problem in tropical areas is cloud cover: satellite images are rarely free of clouds, and the automated process in CLASlite (based on thermal band) is often not sufficient and does not completely mask out all clouds or pixels contaminated by clouds and shadows. To overcome this problem, several images were processed for each year. The areas masked by clouds in one image were replaced by

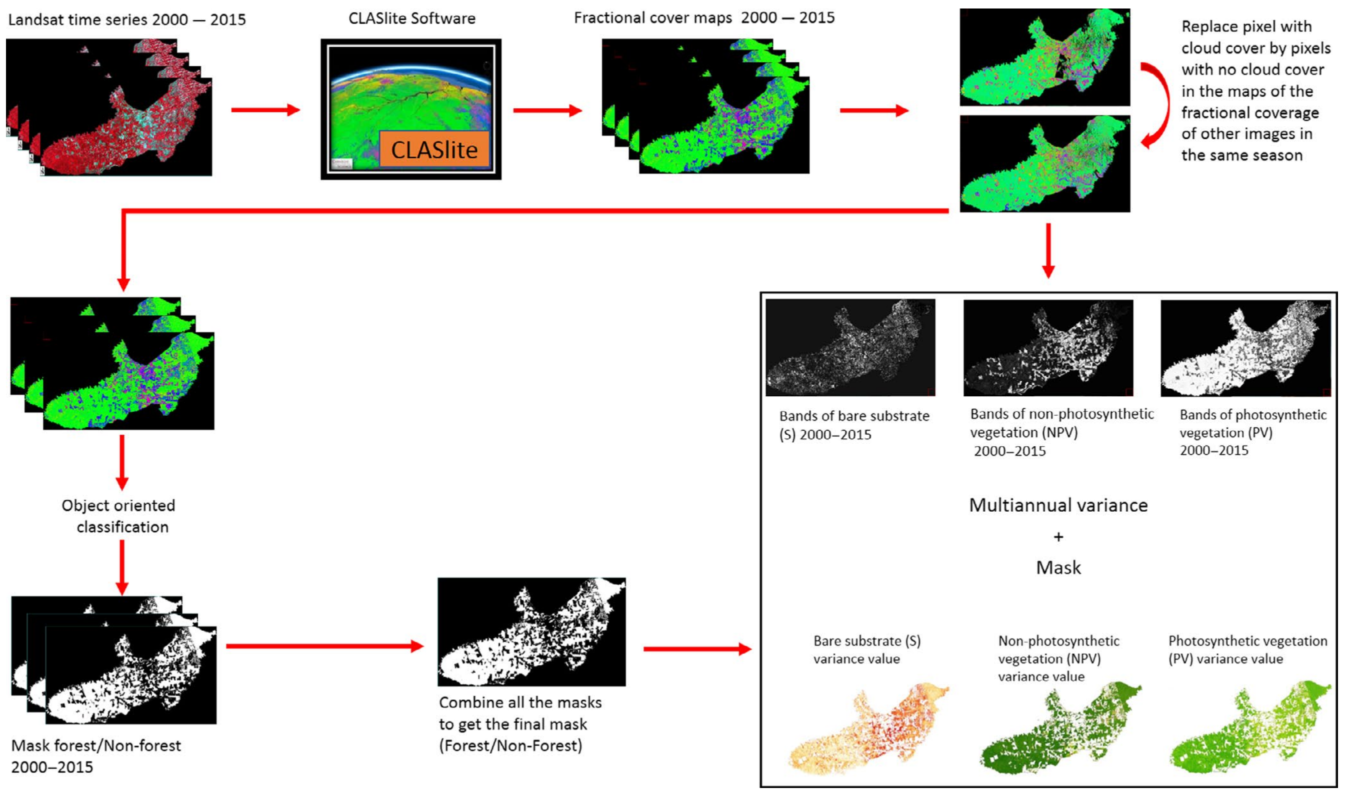

FIGURE 2 CLASlite software processing of Landsat images for the assessment of photosynthetic vegetation, non-photosynthetic vegetation, and bare substrate (S) bands in a multiannual period, and non-forest mask building from CLASlite results [Colour figure can be viewed at wileyonlinelibrary.com]

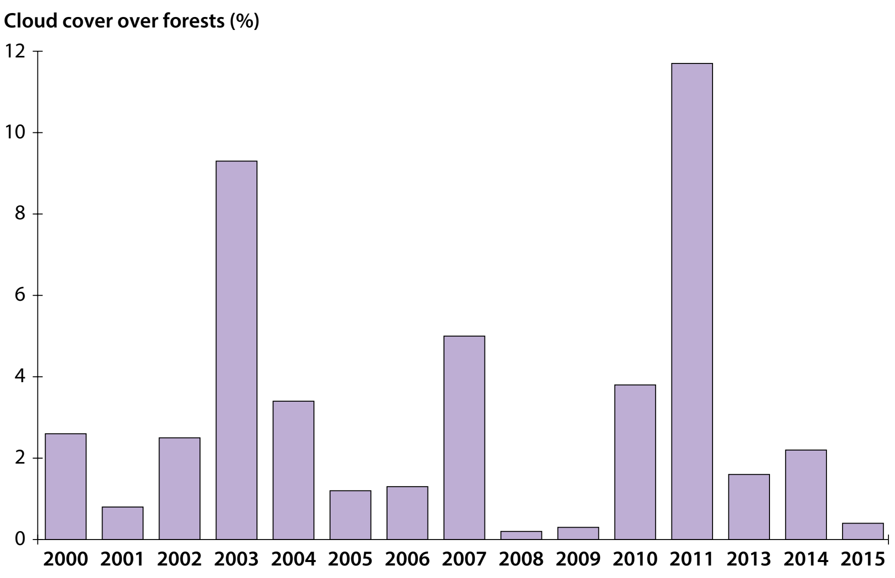

FIGURE 3 Remaining cloud cover over the forested area in Paragominas municipality [Colour figure can be viewed at wileyonlinelibrary.com]

the results of other images acquired in the same season over the same area with no cloud cover. Despite cloud correction, some areas remain masked with cloud (Figure 3), they appear as non-forest areas in white (Figure 4). A composite image was created for each year. A total of 110 images had to be downloaded to cover the entire municipality during the dry season. Even so, it was impossible to build the 2012 map, because the cloud cover was too extensive in all images in that year. 2011 was also very cloudy and was consequently not used at the municipal scale, but local results at plot scale with no cloud cover were used for analysis.

3.3 | Building a primary forest mask

Building a primary forest mask was essential to ensure the S, PV and NPV indicators were only applied in primary forest area. Primary

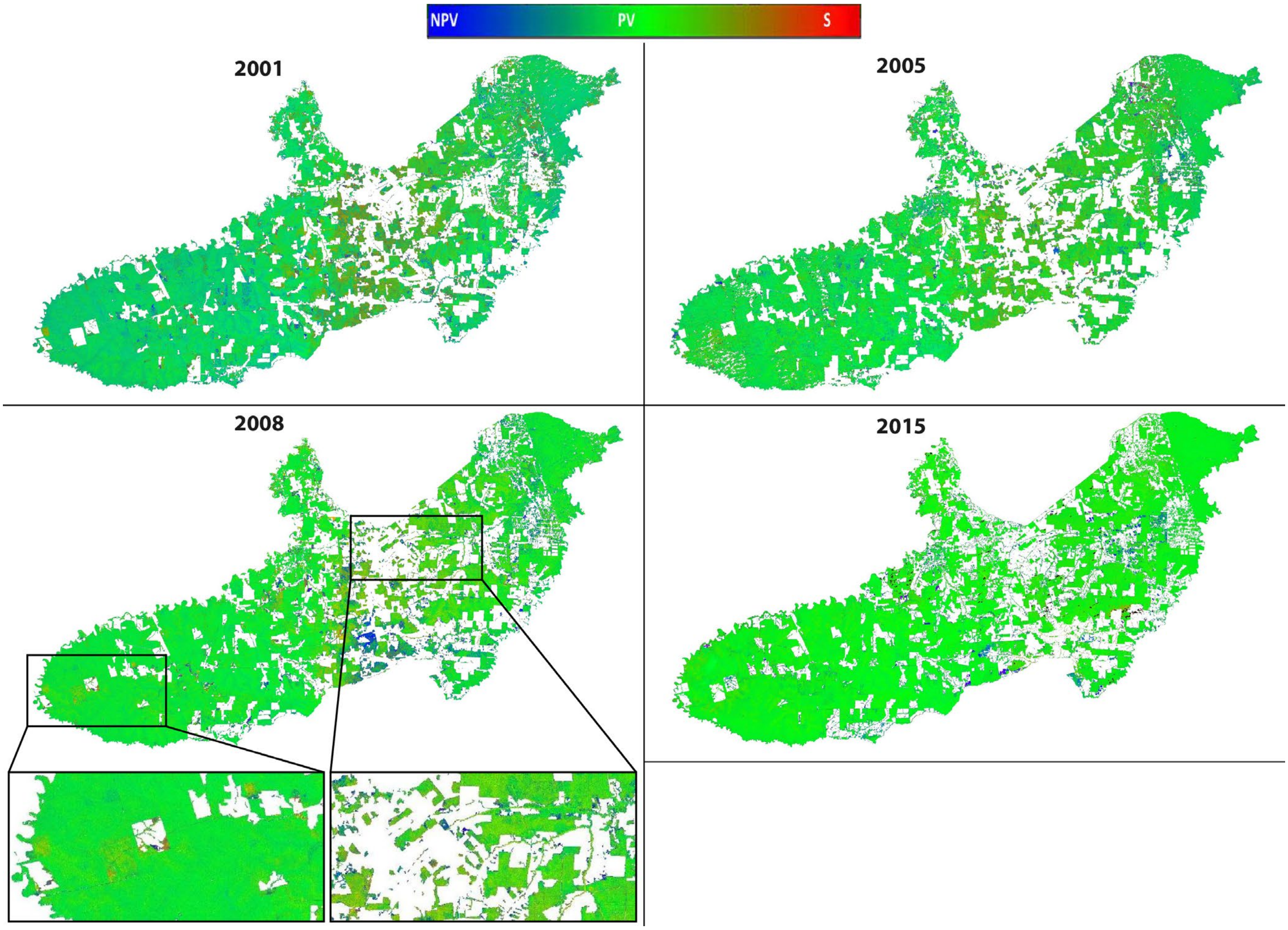

FIGURE 4 Four annual fractional cover maps (2001, 2005, 2008 and 2015) processed with CLASlite software using Landsat images, zooming in on two zones in the 2008 fractional cover map [Colour figure can be viewed at wileyonlinelibrary.com]

forest has to be clearly distinguished from secondary forests, reforested areas (particularly planting of trees such as eucalyptus, which is common in the Brazilian Amazon) and pasture invaded by shrubs. Fractional covers from CLASlite were processed to build non-forest masks for Landsat imagery for each year from 2000 to 2015 (except 2012) using the object-oriented classification method (Figure 2). The primary forest mask for each year was built with the Example Based Feature Extraction method in ENVI 5.0. The method proceeds first by segmentation, which consists in dividing the image into discreet objects by finding edges and grouping pixels into regions; a critical parameter at this stage is selecting the minimum segment size to merge the segments. Secondly, we chose the number of segments for each feature class and identified segments that are representative of each feature class in Google Earth or Landsat images by visual interpretation: we defined 20–25 forest segments (the number varied with the year), from 30–40 non-forest segments and 5–10 cloud segments (resulting from the identification previously carried out with CLASlite). Thirdly, we applied the Support Vector Machine Classification Method based on spectral, texture and spatial criteria (ENVI, 2008, p. 78).

The multi-annual mask was based on the rule that a pixel classified as non-forest in one year remains non-forest for the whole period, which normally leads to the exclusion of secondary forest or tree plantations that are less than 15 years old.

During the field trip, GPS points were taken in primary forest (144 points) and non-primary forest or non-forest areas (692 points). Primary forest GPS points were distinguished visually from plantation trees and from secondary forest, which had a different structure with homogeneous tree size, with no old dominant trees and with only one or two vegetation strata. The GPS points were used to assess the accuracy of the primary forest mask by calculating the Kappa index, which reflects the difference between actual agreement and the agreement expected by chance.

3.4 | Analysis of the fractional cover maps with CLASlite

To get information on annual disturbances, we used the annual fractional cover maps of the municipality. The fractional cover maps reveal the location of the disturbance events. The fractional cover maps were further used at the pixel, plot and municipal scale by using respectively NPV value, mean NPV value and NPV class fractional areas.

To get information on the state of degradation of the forest in 2015, we used ArcGIS Spatial Analyst to compute variance in the annual value at the pixel level of the NPV over the period 2000 to 2015. We assumed that NPV in a forest that had undergone little or no disturbance is small and hardly varies over the years, while repeated disturbance factors such as overlogging, fire and charcoal production will lead to a succession of growth stages and decline stages in NPV. Repeated disturbances would result in more variance in NPV over several years. We therefore assumed that the greater the variance, the more degraded the forest. The distribution of NPV variance was processed in the plots according to the four types of disturbance and the non-degraded forest plots.

4 | RESULTS

4.1 | Primary forest cover in Paragominas

In 2015, the total area of primary forest was 12,767 km^2, representing 65.8% of the municipal area. The accuracy assessment is very good as 97.9% of the GPS points measured in the forest were found in the forest mask; also 98.3% of the GPS points measured in non-forest areas were found in the non-forest mask.

4.2 | Annual maps of the fractional cover representing forest disturbances

Within the mask of primary forest, CLASlite analysis enabled mapping of the forest degradation over time series (Figures 4 and 5). In 2001, a meridian strip with mixed colors expressing significant proportions of S and NPV appeared in the central part of the municipality near the main roads, showing some disturbance; high NPV values (in blue) were diffuse in the western and northeastern part. In 2005, disturbance appeared to be reduced with less diffuse blue and mixed colors and more concentrated and isolated blue patches, mainly in the central and in the northeastern parts. High values of NPV were recorded in 2008 in the central part and in some patches of forest surrounded by non-forested area, while light green dominated the western and northeastern parts. In 2015, the majority of the central part was light green, representing little disturbance; only a few patches in this area and in the northeastern part were dark blue, representing a concentration of disturbances. In all the years, a halo of mixed color or blue appeared at the margins of forest patches, resulting from disturbances near opened areas.

4.3 | Forest degradation trajectories

Figure 6 shows changes in the three CLASlite bands in a 3 pixel × 3 pixel window around a selective logging gap. Two timber harvesting campaigns were clearly revealed by a sharp rise in NPV in 2001 and in 2013. A smaller increase can be observed from 2009 to 2010, which may be due to tree mortality or some other unknown event. Timber harvesting affected the central pixel and its neighbors. As a result of the 2001 disturbance and subsequent regrowth, the average NPV value in the nine pixels decreased slowly up to 2008 following a progressive trend. The S band showed short peaks without following a trend. Except in 2010, the S peaks were not correlated with NPV peaks.

Figure 7 shows the NPV values during the study period for the five disturbance types representing undisturbed forest used as the local benchmark (five plots per type). Results revealed low variability of the mean NPV in undisturbed forest. Among the degraded plots, the highest mean NPV values were found in the burned forest area, with several fire events in 2006, 2008, 2011 and 2015. The NPV returned to a normal value after two or three years depending on the plot. Thus, fire appears to have the strongest consequences on the NPV for the forest. Overlogging for charcoal production in

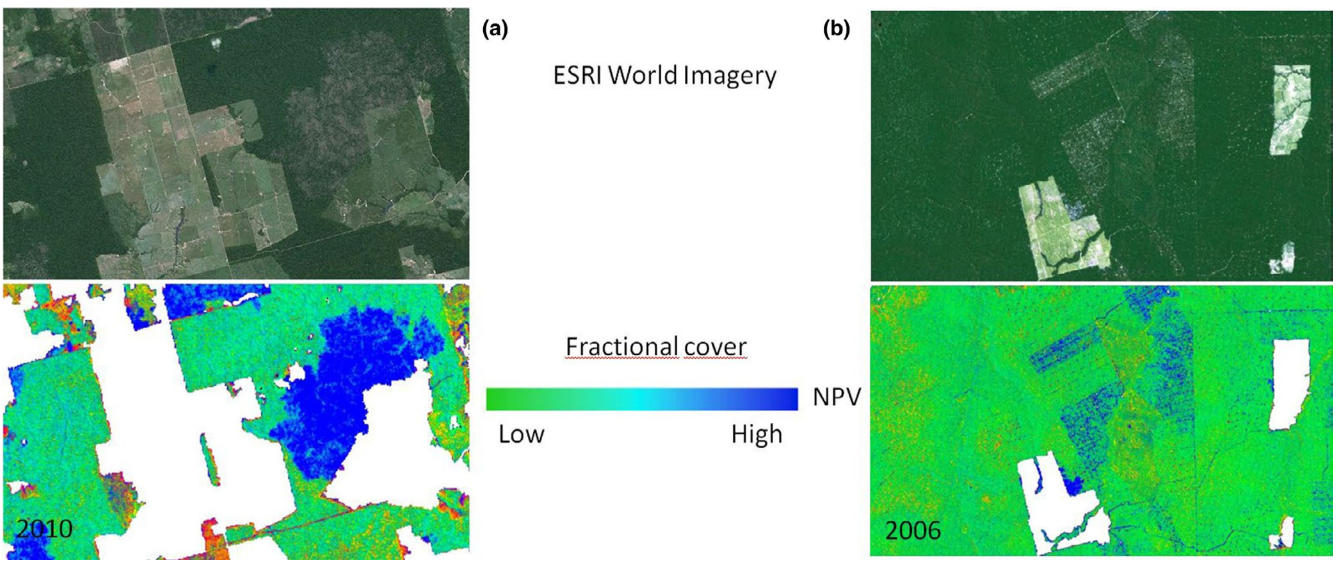

FIGURE 5 Forest degradation patterns in Paragominas observed via non-photosynthetic vegetation (NPV) fractional cover. (a) Zonal disturbance (fuelwood gathering) with homogeneous distribution of non-photosynthetic vegetation in the degraded area and (b) selective logging, with roads and regularly shaped gaps in the plots visible in the NPV fractional cover map [Colour figure can be viewed at wileyonlinelibrary.com]

FIGURE 6 Fractional cover (in %) of bare substrate (S), photosynthetic vegetation (PV) and non-photosynthetic vegetation (NPV) during the period 2000–2015 for a 3 pixel × 3 pixel window; the pixel at the center of the window was affected by a logging gap in 2001 and 2013 [Colour figure can be viewed at wileyonlinelibrary.com]

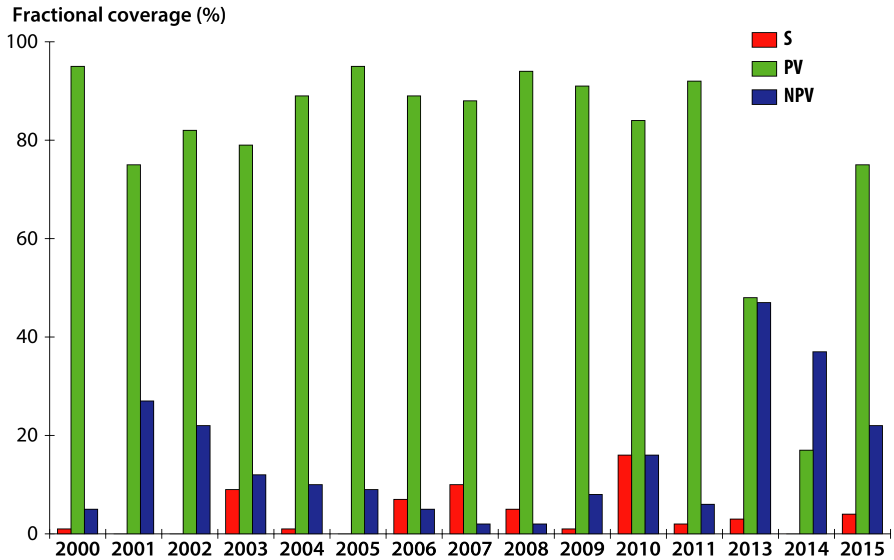

2010 led to a slightly lower mean NPV value compared to fire and its consequences lasted for one to three years. In the selected plots of overlogged forest (no management plan), logging activity was higher before 2004. The consequences of overlogging with no management plan lasted between one and two years. The activity with the least impact was selective logging with a sustainable management plan: the logging had little impact on the mean NPV value and all effects disappeared in a year. The S mean results for the plots are not presented because, as seen at the pixel scale (Figure 6), this fractional band rapidly disappears.

4.4 | NPV variance

4.4.1 | Validation of the NPV variance as a degradation indicator through field observations

Figure 8 shows that the median values and the distribution of NPV variance differ in the five forest degradation trajectories. The NPV variance was lowest for undisturbed forest and gradually increased for selectively logged forest (with a management plan), overlogged forests (no management plan), overlogged forest for charcoal production and burned forest. The NPV variance showed the difference in the intensity of the impacts of the disturbance on the forest over a long period.

4.4.2 | Distribution of forest degradation at the municipal scale

The resulting map shows the pixel NPV variance for the whole municipality over the period 2000–2015. NPV variance was not homogeneous in the study area (Figure 9): the most degradation was observed in a central meridian strip near the main paved road, in an extended northeastern area with a mosaic of forest/non-forest patches, and some places in the northwest of the municipality appear to be more degraded; while in an extended western part, in some large patches in the east and in the indigenous reserve in the far northeast, forests appear to be better preserved.

4.4.3 | Changes in forest degradation at the municipal scale

The highest NPV values are expected to represent the most severe disturbance phenomena. Changes in the extent of degraded areas in annual time steps are an indicator of changes in disturbance at the municipal scale. Considering the relative extent of higher NPV values (NPV fractional cover >15%, Figure 10), 2006 and 2008 were the years with the most severe disturbances. In 2009 and 2010, disturbances appeared to occur less frequently. In 2013, 2014 and 2015, the area with high NPV values increased as a large proportion of primary forest area was disturbed. The lowest class of NPV values did not display the same dynamics: their extent has increased since 2004, particularly since 2013.

5 | DISCUSSION

Spectral mixture analysis has proven its efficiency in assessing the regional distribution of forest disturbance based on public data (Chicas et al., 2016; Reimer, Asner, & Joseph, 2015). One advantage of CLASlite is that it separates the phenological bands that are useful for detecting disturbance. It performs separate quantitative analysis of each band at the pixel scale. The series of CLASlite fractional cover maps showed that it is possible to identify disturbances at pixel scale. As reported in other work, CLASlite results enable detection of the gaps created by selective logging in rainforest (Monteiro et al., 2003; Tritsch et al., 2016). For selective logging, CLASlite results provide information including the density and the size of the gaps in a forest plot, the logging year, logging intensity (indicated by the size of the gaps), the time needed for secondary vegetation to close the gap and the time between two selective logging campaigns in the same area. Additionally, the results

FIGURE 7 Mean values of non-photosynthetic vegetation for the five reference plots of undisturbed forest and each of the four degradations [Colour figure can be viewed at wileyonlinelibrary.com]

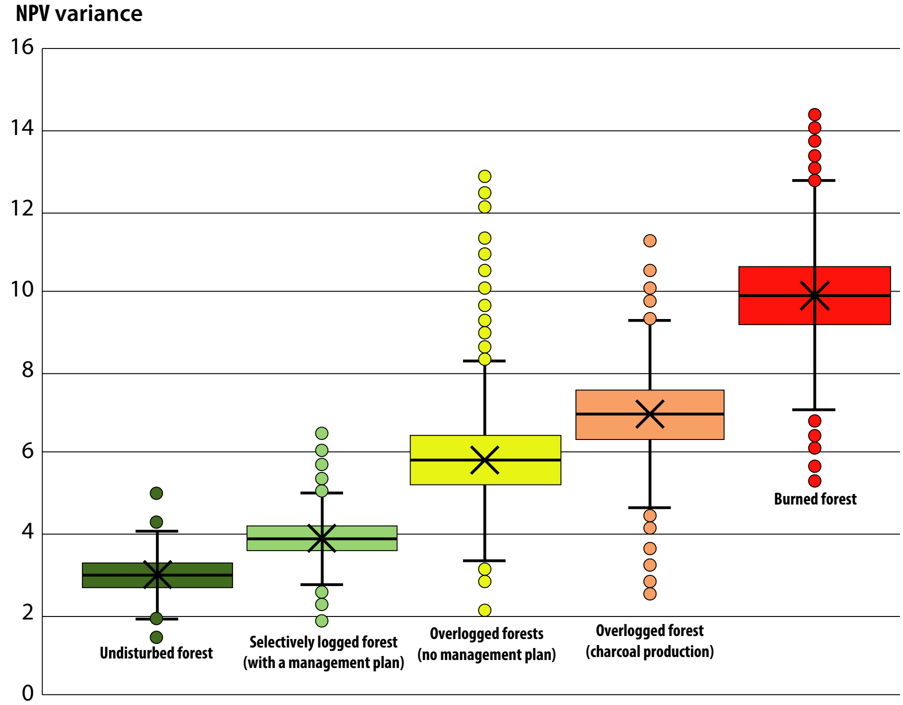

FIGURE 8 Variance of non-photosynthetic vegetation calculated for undisturbed forest and each of the four degradation types; the boxplots report the median value and the distribution of variances computed for each pixel of the reference plots over the period 2000–2015 [Colour figure can be viewed at wileyonlinelibrary.com]

of our study show that the NPV can be used to identify and characterize other types of disturbance such as forest fires and gathering of fuelwood. As pointed out by Cochrane and Souza, the NPV band can be used to map burned forests and several levels of forest disturbance by fire (Cochrane, 1998). However, artifacts can occur at the edge of the forest, particularly in riverine forests or in mosaics of smallholder farms due to the presence of mixed pixels containing trees and pastures or crops, which can increase the NPV values. The sensitivity of NPV in narrow forest patches in the landscape requires further analysis.

Knowing forestry practices, one can assume that the dead wood left following timber harvesting, or a tree falling on the surrounding vegetation, takes several years to disappear. The presence of bare substrate is due to the passage of the forestry machinery used to transport timber. By analyzing time series, we show that NPV can also be used to monitor the trajectory of forest recovery through the progressive decline of the NPV band at pixel and plot scale, while the S band lasts a shorter time in the rainforest because secondary vegetation rapidly closes the vegetation gap created by the disturbance events (Figure 6). As shown by Asner et al. (2004), approximately 50% of the canopy opening caused by selective logging closes in one year of regrowth following timber harvests. For this reason, the S band was no longer used in the analysis. The trajectories of the NPV values showed that the gaps closed between one and four years after the disturbance; this result is in agreement with that obtained by Asner, Keller, Lentini, Merry, & Souza (2009). The speed of NPV regression is linked to the intensity and type of disturbance. Large gaps in the forest are usually slow to recover and thus have long-lasting effects (Asner et al., 2006). However, our results may be disrupted by the effect of climate variability on the proportion of NPV. Dry years are assumed to generate senescent vegetation and partial leaf fall that may reveal NPV such as wood and litter. On the other hand, the driest years in the Amazonian region, 2005, 2010 and 2015, were not associated with a notable increase in the extent of areas with high NPV (Figure 10).

Most available remote-sensing methods have been used to detect disturbance events but their cumulative effects were not evaluated. In the present study, NPV variance was used as a multi-annual aggregation indicator to assess the medium- and long-term impacts of the disturbance processes. The results showed that the higher the NPV variance, the more degraded the forest. The highest NPV variance was observed in the case of fire. Fire causes more drastic changes to the structure of forest than selective logging, in burned forest there is a severe collapse of forest biomass, jeopardizing natural regeneration and increasing the susceptibility of the forests to subsequent fires (Cochrane & Schulze, 1999).

The spatial distribution of pixel NPV variance at the municipal scale appears to be linked to the distance from the main roads and the proximity of cleared areas (pasture, cropland, urbanization) that damage the forest, such as uncontrolled fires that facilitate the extraction of timber and charcoal. This may be reflected by spatial differentiation between non-protected areas with increasing degradation near the main roads, and agricultural land use, and the protected forest in the western part with a management plan and the indigenous reserve in the northeastern part.

The dynamics of forest disturbances at the municipal scale also revealed marked differences in deforestation dynamics. In Paragominas, deforestation decreased from 334 km^2 in 2005 to an average annual deforestation of 33 km^2 over the period 2010 to 2015 (source: PRODES database, INPE), due to the stricter application of the Forest Code and the Green Municipality commitment (Laurent et al., 2017; Piketty et al., 2015). However, the remaining primary forests are undergoing degradation that is affecting a larger area than deforestation. In a region in Mato Grosso, Grecchi et al.

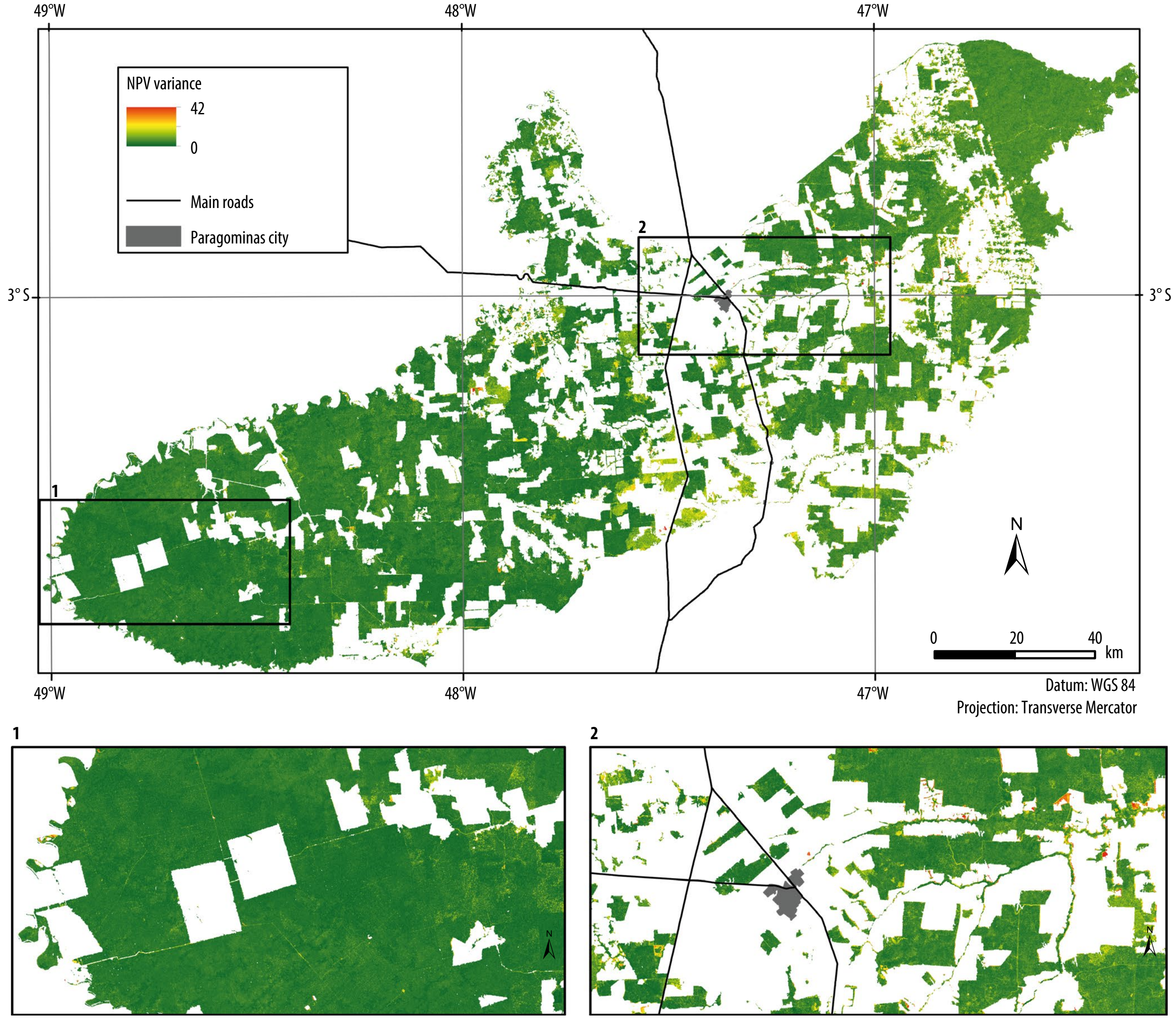

FIGURE 9 Mapping of the variance of non-photosynthetic vegetation calculated over the period 2000–2015 in the municipality of Paragominas, with a detailed view of two zones [Colour figure can be viewed at wileyonlinelibrary.com]

(2017) also identified areas affected by greater disturbances caused by selective logging than by deforestation and an increasing ratio between annual rates of disturbance and annual rates of deforestation during the period 2000–2015. Today, in these study areas, which are representative of the Amazonian agricultural frontier, degradation no longer leads to deforestation, as observed in the past (Gibbs et al., 2010; Nepstad et al., 1999). The two processes are decoupled, as we also observed in the present study.

In Paragominas, a sharp increase in forest disturbance has been under way since 2013 with 625 km² of new highly disturbed area (identified by a fractional cover of NPV higher than 20%), equivalent to 4.9% of the municipal primary forest area (Figure 10). The results obtained using the NPV fractional cover method are considerably higher than those obtained using DEGRAD (except for 2010, Figure 11), and can be explained by the spatial resolution of the NPV fractional cover method, which detects disturbances affecting areas as small as 900 m², whereas DEGRAD only identifies disturbed areas larger than 62,500 m². However, a spatial overlay of the two maps showed that the two methods converged: the mean fractional cover of NPV was systematically greater inside the degraded polygons identified with the INPE method than outside (Figure 12).

6 | CONCLUSION

The results of the present study highlight the need to not only consider the actual deforestation process when assessing tropical forest conservation. Even in a municipality considered as a model for sustainable development in the Amazon, where the rate of deforestation is decreasing, degradation continues and is even on the

FIGURE 10 Percentage of pixels in five classes of non-photosynthetic vegetation fractional cover value in the forested area of the municipality of Paragominas; distribution is displayed for each year over the period 2000–2015 [Colour figure can be viewed at wileyonlinelibrary.com]

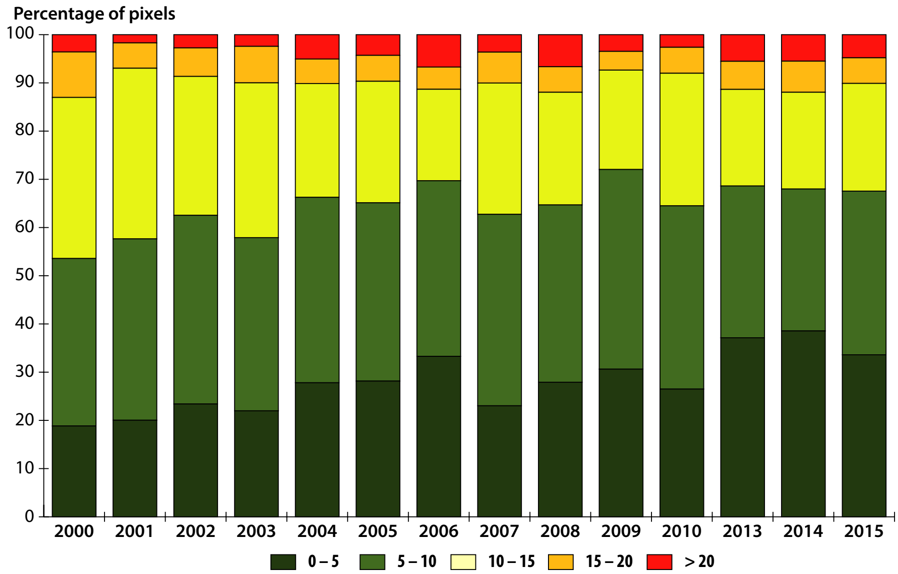

FIGURE 11 Assessment of area of forest degradation in Paragominas municipality estimated using the DEGRAD–INPE method (www.obt.inpe.br/OBT/assuntos/programas/amazonia/degrad) and the CLASlite method (this study); only pixels with the highest values of NPV fractional cover (>20%) were selected [Colour figure can be viewed at wileyonlinelibrary.com]

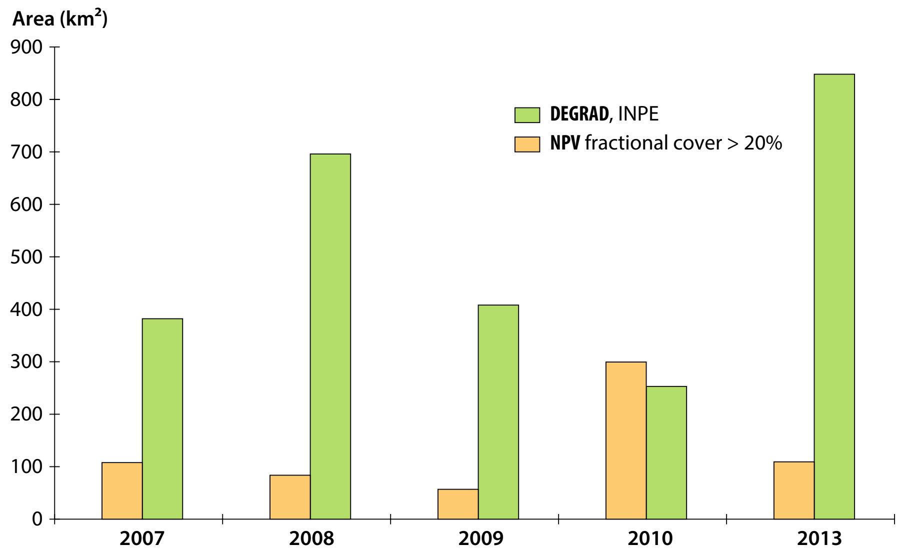

FIGURE 12 Mean value for non-photosynthetic vegetation calculated for all the pixels inside and outside the polygons recorded by DEGRAD–INPE mapping [Colour figure can be viewed at wileyonlinelibrary.com]

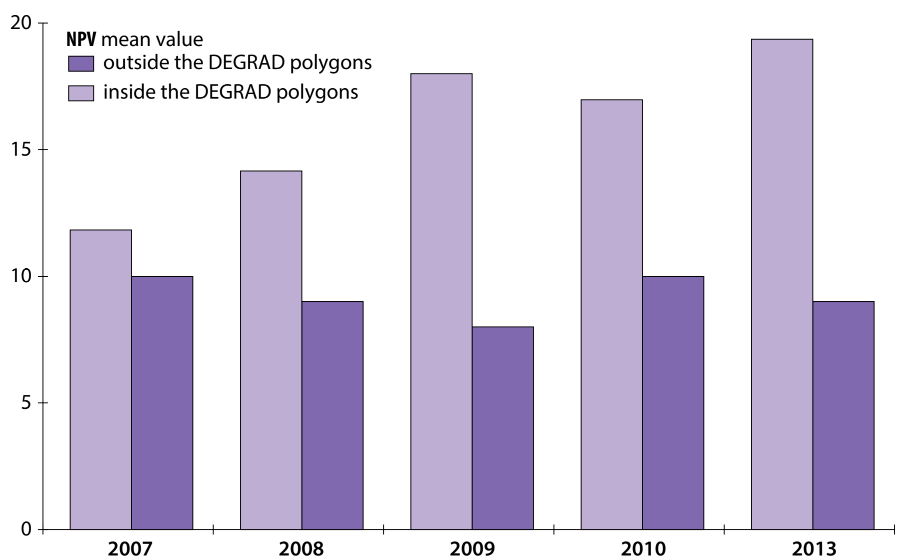

increase, with major consequences for biodiversity, carbon sequestration and other ecosystem services. There is thus an urgent need for the monitoring and regulation of forest degradation. The NPV fractional cover is an appropriate tool for mapping forest disturbance events, as well as for differentiating between causes such as selective logging and forest fire. The aggregation of fractional cover during time series by multi-annual NPV variance makes it possible to map medium- and long-term degradation and their relation with intensity and frequency of forest disturbances.

ACKNOWLEDGEMENTS

The research was conducted with the financial support of the French *Agence Nationale de la Recherche* (ANR), ECOTERA Project "Eco-efficiences et développement territorial en Amazonie brésilienne"; ANR-13-AGRO-0003) and the European Union, which funded the H2020-MSCA-RISE-2015 ODYSSEA project. We are grateful to Cikel Verde who gave us access to their property and provided information on forest management plans as well as technical assistance. We thank Sébastien Angonnet for his help in producing the graphics.

DATA AVAILABILITY

The data that support the findings of this study are available from the corresponding author (FL) upon reasonable request.

ORCID

François Laurent https://orcid.org/0000-0002-3833-2022

REFERENCES

Aguiar, A. P. D., Vieira, I. C. G., Assis, T. O., Dalla-Nora, E. L., Toledo, P. M., Oliveira Santos-Junior, R. A., … Ometto, J. P. H. (2016). Land use change emission scenarios: anticipating a forest transition process in the Brazilian Amazon. *Global Change Biology*, *22*(5), 1821–1840. https://doi.org/10.1111/gcb.13134

Alves, D. S., Morton, D. C., Batistella, M., Roberts, D. A., & Souza, C. Jr (2009). The changing rates and patterns of deforestation and land use in Brazilian Amazonia. In M. Keller, M. Bustamante, J. Gash & P. Silva Dias (Eds.), *Amazonia and Global Change. Geophysical Monograph Series*, Vol. *186* (pp. 1–9). Washington, DC: American Geophysical Union. https://doi.org/10.1029/2009gm000902

Andrade, F. S. (2011). Variabilidade da precipitação pluviométrica de um município do estado do Pará. *Engenharia Ambiental - Espírito Santo do Pinhal*, *8*(4), 138–145.

Asner, G. P., Broadbent, E. N., Oliveira, P. J. C., Keller, M., Knapp, D. E., & Silva, J. N. M. (2006). Condition and fate of logged forests in the Brazilian Amazon. *Proceedings of the National Academy of Sciences*, *103*(34), 12947–12950. https://doi.org/10.1073/pnas.0604093103

Asner, G. P., Keller, M., Lentini, M., Merry, F., & Souza, C. (2009). Selective logging and its relation to deforestation. In M. Keller, M. Bustamante, J. Gash & P. Silva Dias (Eds.), *Amazonia and Global Change. Geophysical Monograph Series*, Vol. *186* (pp. 25–42). https://doi.org/10.1029/2008gm000723

Asner, G. P., Keller, M., Pereira, R. Jr, Zweede, J. C., & Silva, J. N. M. (2004). Canopy damage and recovery after selective logging in Amazonia: field and satellite studies. *Ecological Applications*, *14*(sp4), 280–298. https://doi.org/10.1890/01-6019

Asner, G. P., Knapp, D., Balaji, A., & Paez-Acosta, G. (2009). Automated mapping of tropical deforestation and forest degradation: CLASlite. *Journal of Applied Remote Sensing*, *3*(1), 033543. https://doi.org/10.1117/1.3223675

Asner, G. P., Knapp, D. E., Broadbent, E. N., Oliveira, P. J. C., Keller, M., & Silva, J. N. (2005). Selective logging in the Brazilian Amazon. *Science*, *310*(5747), 480–482. https://doi.org/10.1126/science.1118051

Asner, G. P., Rudel, T. K., Aide, T. M., Defries, R., & Emerson, R. (2009). A contemporary assessment of change in humid tropical forests. *Conservation Biology*, *23*(6), 1386–1395. https://doi.org/10.1111/j.1523-1739.2009.01333.x

Baccini, A., Walker, W., Carvalho, L., Farina, M., Sulla-Menashe, D., & Houghton, R. A. (2017). Tropical forests are a net carbon source based on aboveground measurements of gain and loss. *Science*, *358*(6360), 230–234. https://doi.org/10.1126/science.aam5962

Bourgoin, C., Blanc, L., Bailly, J.-S., Cornu, G., Berenguer, E., Oszwald, J., … Gond, V. (2018). The potential of multisource remote sensing for mapping the biomass of a degraded Amazonian forest. *Forests*, *9*(6), 303. https://doi.org/10.3390/f9060303

Bustamante, M. M. C., Roitman, I., Aide, T. M., Alencar, A., Anderson, L. O., Aragão, L., … Vieira, I. C. G. (2016). Toward an integrated monitoring framework to assess the effects of tropical forest degradation and recovery on carbon stocks and biodiversity. *Global Change Biology*, *22*(1), 92–109. https://doi.org/10.1111/gcb.13087

Cardille, J. (2003). Agricultural land-use change in Brazilian Amazônia between 1980 and 1995: Evidence from integrated satellite and census data. *Remote Sensing of Environment*, *87*(4), 551–562. https://doi.org/10.1016/j.rse.2002.09.001

Chicas, S. D., Omine, K., & Saqui, P. (2016). CLASlite algorithms and social surveys to asses and identify deforestation and forest degradation in Toledo's protected areas and forest ecosystems, Belize. *Applied Geography*, *75*, 144–155. https://doi.org/10.1016/j.apgeog.2016.08.012

CLASlite (2014). *CLASlite Forest Monitoring Technology. Version 3.2 user guide*. Stanford, CA: Carnegie Institution for Science, Department of Global Ecology.

Cochrane, M. A. (1998). Linear mixture model classification of burned forests in the Eastern Amazon. *International Journal of Remote Sensing*, *19*(17), 3433–3440. https://doi.org/10.1080/014311698214109

Cochrane, Mark. A., & Schulze, M. D. (1999). Fire as a recurrent event in tropical forests of the eastern Amazon: effects on forest structure, biomass, and species composition. *Biotropica*, *31*(1), 2–16. https://doi.org/10.1111/j.1744-7429.1999.tb00112.x

DeVries, B., Decuyper, M., Verbesselt, J., Zeileis, A., Herold, M., & Joseph, S. (2015). Tracking disturbance-regrowth dynamics in tropical forests using structural change detection and Landsat time series. *Remote Sensing of Environment*, *169*, 320–334. https://doi.org/10.1016/j.rse.2015.08.020

Diniz, C. G., Souza, A. A. A., Santos, D. C., Dias, M. C., da Luz, N. C., de, Moraes, D. R. V., … Adami, M. (2015). DETER-B: The new Amazon near real-time deforestation detection system. *IEEE Journal of Selected Topics in Applied Earth Observations and Remote Sensing*, *8*(7), 3619–3628. https://doi.org/10.1109/jstars.2015.2437075

Dlamini, W. M. (2017). Mapping forest and woodland loss in Swaziland: 1990–2015. *Remote Sensing Applications: Society and Environment*, *5*, 45–53. https://doi.org/10.1016/j.rsase.2017.01.004

ENVI (2008). Feature extraction module version 4.6 (p. 78). ITT Visual Information Solutions. Retrieved from http://www.harrisgeospatial.com/portals/0/pdfs/envi/feature_extraction_module.pdf

Ewers, R. M., Laurance, W. F., & Souza, C. M. (2008). Temporal fluctuations in Amazonian deforestation rates. *Environmental Conservation*, *35*(4), 303–310. https://doi.org/10.1017/s0376892908005122

FAO (2002). *Proceedings: Second expert meeting on harmonizing forest-related definitions for use by various stakeholders*. Rome, Italy: FAO.

FAO (2011). Assessing forest degradation: Towards the development of globally applicable guidelines. Forest Resources Assessment Working Paper No. 177. Rome: FAO. Retrieved from http://www.fao.org/3/a-i2479e.pdf

Fearnside, P. (2017). Business as Usual: A Resurgence of Deforestation in the Brazilian Amazon. *Yale Environment 360*. Retrieved from https://e360.yale.edu/features/business-as-usual-a-resurgence-of-deforestation-in-the-brazilian-amazon

Ferreira, J., Blanc, L., Kanashiro, M., Lees, A. C., Bourgoin, C., de, Veloso Freitas, J., … Sist, P. (2015). Degradação florestal na Amazônia: como ultrapassar os limites conceituais, científicos e técnicos para mudar esse cenário. Documentos No. 413 (p. 29). Belém, Brazil: Embrapa Amazônia oriental. Retrieved from www.embrapa.br/amazonia-oriental/publicacoes

Garcia, R. A., Soares-Filho, B. S., & Sawyer, D. O. (2007). Socioeconomic dimensions, migration, and deforestation: An integrated model of territorial organization for the Brazilian Amazon. *Ecological Indicators*, *7(3)*, 719–730. https://doi.org/10.1016/j.ecolind.2006.08.003

Gerwing, J. (2002). Degradation of forests through logging and fire in the eastern Brazilian Amazon. *Forest Ecology and Management*, *157(1–3)*, 131–141. https://doi.org/10.1016/s0378-1127(00)00644-7

Gibbs, H. K., Munger, J., L'Roe, J., Barreto, P., Pereira, R., Christie, M., … Walker, N. F. (2016). Did ranchers and slaughterhouses respond to zero-deforestation agreements in the Brazilian Amazon? . *Conservation Letters*, *9*(1), 32–42. https://doi.org/10.1111/conl.12175

Gibbs, H. K., Ruesch, A. S., Achard, F., Clayton, M. K., Holmgren, P., Ramankutty, N., & Foley, J. A. (2010). Tropical forests were the primary sources of new agricultural land in the 1980s and 1990s. *Proceedings of the National Academy of Sciences*, *107*(38), 16732–16737. https://doi.org/10.1073/pnas.0910275107

Grecchi, R. C., Beuchle, R., Shimabukuro, Y. E., Aragão, L. E. O. C., Arai, E., Simonetti, D., & Achard, F. (2017). An integrated remote sensing and GIS approach for monitoring areas affected by selective logging: A case study in northern Mato Grosso, Brazilian Amazon. *International Journal of Applied Earth Observation and Geoinformation*, *61*, 70–80. https://doi.org/10.1016/j.jag.2017.05.001.

Hosonuma, N., Herold, M., De Sy, V., De Fries, R. S., Brockhaus, M., Verchot, L., … Romijn, E. (2012). An assessment of deforestation and forest degradation drivers in developing countries. *Environmental Research Letters*, *7*(4), 044009. https://doi.org/10.1088/1748-9326/7/4/044009

INPE (2008). Relatório Monitoramento da cobertura florestal da Amazônia por satélites: Sistemas PRODES, DETER, DEGRAD e QUEIMADAS 2007–2008. São José dos Campos, Brazil: INPE, Ministério da Ciência e Tecnologia.

INPE (2010). Municipal-level PRODES dataset. National Institute for Space Research (INPE), available at http://www.dpi.inpe.br/ prodesdigital/prodesmunicipal.php.

ITTO (2002). *ITTO guidelines for the restoration, management and rehabilitation of degraded and secondary tropical forests*. Yokohama, Japan: ITTO.

Lamb, D., & Gilmour, D. (2003). *Rehabilitation and restoration of degraded forests*. Gland, Switzerland: IUCN.

Lambin, E. F. (1999). Monitoring forest degradation in tropical regions by remote sensing: some methodological issues. *Global Ecology and Biogeography*, *8*(3–4), 191–198. https://doi.org/10.1046/j.1365-2699.1999.00123.x

Laurent, F., Arvor, D., Daugeard, M., Osis, R., Tritsch, I., Coudel, E., … Messner, F. (2017). Le tournant environnemental en Amazonie : Ampleur et limites du découplage entre production et déforestation. *EchoGéo*, *41*. https://doi.org/10.4000/echogeo.15035

Laurent, F., Poccard-Chapuis, R., Plassin, S., & Pimentel Martinez, G. (2016). Soil texture derived from topography in North-eastern Amazonia. *Journal of Maps*, *13*(2), 109–115. https://doi.org/10.1080/17445647.2016.1266524

Matricardi, E. A. T., Skole, D. L., Cochrane, M. A., Qi, J., & Chomentowski, W. (2005). Monitoring selective logging in tropical evergreen forests using Landsat: multitemporal regional analyses in Mato Grosso, Brazil. *Earth Interactions*, *9*(24), 1–24.

Matricardi, E. A. T., Skole, D. L., Pedlowski, M. A., Chomentowski, W., & Fernandes, L. C. (2010). Assessment of tropical forest degradation by selective logging and fire using Landsat imagery. *Remote Sensing of Environment*, *114*(5), 1117–1129. https://doi.org/10.1016/j.rse.2010.01.001

Monteiro, A. L., Souza Jr, C. M., & Barreto, P. (2003). Detection of logging in Amazonian transition forests using spectral mixture models. *International Journal of Remote Sensing*, *24*(1), 151–159. https://doi.org/10.1080/01431160305008

Nepstad, D., McGrath, D., Stickler, C., Alencar, A., Azevedo, A., Swette, B., … Hess, L. (2014). Slowing Amazon deforestation through public policy and interventions in beef and soy supply chains. *Science*, *344*(6188), 1118–1123. https://doi.org/10.1126/science.1248525

Nepstad, D. C., Verssimo, A., Alencar, A., Nobre, C., Lima, E., Lefebvre, P., … Brooks, V. (1999). Large-scale impoverishment of Amazonian forests by logging and fire. *Nature*, *398*(6727), 505–508. https://doi.org/10.1038/19066

Oliveira, P. J. C., Asner, G. P., Knapp, D. E., Almeyda, A., Galván-Gildemeister, R., Keene, S., … Smith, R. C. (2007). Land-use allocation protects the Peruvian Amazon. *Science*, *317*(5842), 1233–1236. https://doi.org/10.1126/science.1146324

Piketty, M. G., Poccard-Chapuis, R., Drigo, I., Coudel, E., Plassin, S., … Thâles, M. (2015). Multi-level governance of land use changes in the Brazilian Amazon: lessons from Paragominas, State of Pará. *Forests*, *6*(5), 1516–1536. https://doi.org/10.3390/f6051516

Pinheiro, T. F., Escada, M. I. S., Valeriano, D. M., Hostert, P., Gollnow, F., & Müller, H. (2016). Forest degradation associated with logging frontier expansion in the Amazon: The BR-163 region in southwestern Pará, Brazil. *Earth Interactions*, *20*(17), 1–26. https://doi.org/10.1175/ei-d-15-0016.1

Reimer, F., Asner, G. P., & Joseph, S. (2015). Advancing reference emission levels in subnational and national REDD+ initiatives: A CLASlite approach. *Carbon Balance and Management*, *10*(1), 5. https://doi.org/10.1186/s13021-015-0015-8

Rodrigues, A. S. L., Ewers, R. M., Parry, L., Souza, C. Jr, Veríssimo, A., & Balmford, A. (2009). Boom-and-bust development patterns across the Amazon deforestation frontier. *Science*, *324(5933)*, 1435–1437. https://doi.org/10.1126/science.1174002

Shimabukuro, Y. E., Beuchle, R., Grecchi, R. C., & Achard, F. (2014). Assessment of forest degradation in Brazilian Amazon due to selective logging and fires using time series of fraction images derived from Landsat ETM+ images. *Remote Sensing Letters*, *5*(9), 773–782. https://doi.org/10.1080/2150704X.2014.967880.

Sist, P., Mazzei, L., Blanc, L., & Rutishauser, E. (2014). Large trees as key elements of carbon storage and dynamics after selective logging in the Eastern Amazon. *Forest Ecology and Management*, *318*, 103–109. https://doi.org/10.1016/j.foreco.2014.01.005

Souza, Jr C., & Barreto, P. (2000). An alternative approach for detecting and monitoring selectively logged forests in the Amazon. *International Journal of Remote Sensing*, *21*(1), 173–179. https://doi.org/10.1080/014311600211064

Souza, Jr C., Firestone, L., Silva, L. M., & Roberts, D. (2003). Mapping forest degradation in the Eastern Amazon from SPOT 4 through spectral mixture models. *Remote Sensing of Environment*, *87*(4), 494–506. https://doi.org/10.1016/j.rse.2002.08.002

Souza, Jr C. , Siqueira, J., Sales, M., Fonseca, A., Ribeiro, J., Numata, I., … Barlow, J. (2013). Ten-Year landsat classification of deforestation and forest degradation in the Brazilian Amazon. *Remote Sensing*, *5*(11), 5493–5513. https://doi.org/10.3390/rs5115493

Théry, H. (1997). Routes et déboisement en Amazonie brésilienne: Rondônia 1974-1996. *Mappe Monde*, *97(3)*, 35–40.

Thompson, I. D., Guariguata, M. R., Okabe, K., Bahamondez, C., Nasi, R., Heymell, V., & Sabogal, C. (2013). An operational framework for defining and monitoring forest degradation. *Ecology and Society*, *18*(2), 20.

Tritsch, I., & Arvor, D. (2016). Transition in environmental governance in the Brazilian Amazon: Emergence of a new pattern of socio-economic development and deforestation. *Land Use Policy*, *59*, 446–455. https://doi.org/10.1016/j.landusepol.2016.09.018

Tritsch, I., Sist, P., Narvaes, I. S., Mazzei, L., Blanc, L., Bourgoin, C., … Gond, V. (2016). Multiple patterns of forest disturbance and logging shape forest landscapes in Paragominas, Brazil. *Forests*, *7*(12), 315. https://doi.org/10.3390/f7120315

Velasco Gomez, M. D., Beuchle, R., Shimabukuro, Y., Grecchi, R., Simonetti, D., Eva, H. D., & Achard, F. (2015). A long-term perspective on deforestation rates in the Brazilian Amazon. *ISPRS - International Archives of the Photogrammetry, Remote Sensing and Spatial Information Sciences*, *XL-7/W3*, 539–544. https://doi.org/10.5194/isprsarchives-xl-7-w3-539-2015

Verissimo, A., Barreto, P., Mattos, M., Tarifa, R., & Uhl, C. (1992). Logging impacts and prospects for sustainable forest management in an old Amazonian frontier: The case of Paragominas. *Forest Ecology and Management*, 169–199. https://doi.org/10.1016/0378-1127(92)90099-u

Vermote, E. F., Tanre, D., Deuze, J. L., Herman, M., & Morcette, J.-J. (1997). Second Simulation of the Satellite Signal in the Solar Spectrum, 6S: An overview. *IEEE Transactions on Geoscience and Remote Sensing*, *35*(3), 675–686. https://doi.org/10.1109/36.581987

Xaud, H. A. M., Martins, F. S. R. V., & dos Santos, J. R. (2013). Tropical forest degradation by mega-fires in the northern Brazilian Amazon. *Forest Ecology and Management*, *294*, 97–106. https://doi.org/10.1016/j.foreco.2012.11.036

How to cite this article: Hasan AF, Laurent F, Messner F, Bourgoin C, Blanc L. Cumulative disturbances to assess forest degradation using spectral unmixing in the northeastern Amazon. *Appl Veg Sci*. 2019;22:394–408. https://doi.org/10.1111/avsc.12441